Neuron
Article

A Tyramine-Gated Chloride Channel Coordinates Distinct Motor Programs of a *Caenorhabditis elegans* Escape Response

Jennifer K. Pirri,[1] Adam D. McPherson,[1] Jamie L. Donnelly,[1] Michael M. Francis,[1] and Mark J. Alkema[1,*]
[1]Department of Neurobiology, LRB 717, University of Massachusetts Medical School, 364 Plantation Street, Worcester, MA 01605, USA
*Correspondence: mark.alkema@umassmed.edu
DOI 10.1016/j.neuron.2009.04.013

SUMMARY

A key feature of escape responses is the fast translation of sensory information into a coordinated motor output. In *C. elegans*, anterior touch initiates a backward escape response in which lateral head movements are suppressed. Here, we show that tyramine inhibits head movements and forward locomotion through the activation of a tyramine-gated chloride channel, LGC-55. *lgc-55* mutant animals have defects in reversal behavior and fail to suppress head oscillations in response to anterior touch. *lgc-55* is expressed in neurons and muscle cells that receive direct synaptic inputs from tyraminergic motor neurons. Therefore, tyramine can act as a classical inhibitory neurotransmitter. Activation of LGC-55 by tyramine coordinates the output of two distinct motor programs, locomotion and head movements that are critical for a *C. elegans* escape response.

INTRODUCTION

Biogenic amines play an important role in the modulation of behaviors in a wide variety of organisms. In contrast to the classical biogenic amines, like dopamine or serotonin, roles for trace amines in the nervous system remain elusive. The trace amine, tyramine is found in the nervous system of animals ranging from nematodes to mammals. Tyramine has often been considered as a metabolic byproduct, or intermediate in the biosynthesis, of the classical biogenic amines. However, the characterization of invertebrate and mammalian G protein-coupled receptors that can be activated by tyramine has piqued new interest in the role of tyramine in animal behavior and physiology. The mammalian trace-amine associated receptor TAAR1 has a high affinity for tyramine and β-phenylethylamine and is broadly expressed in the mammalian brain (Borowsky et al., 2001; Miller et al., 2005). Tyramine responsive G protein-coupled receptors have been characterized in fruit flies, locusts, honeybees, silk moths, and nematodes (Blenau et al., 2000; Ohta et al., 2003; Rex et al., 2005; Rex and Komuniecki, 2002; Saudou et al., 1990). However, it is unclear whether tyramine is the endogenous ligand for these receptors and the role of tyramine in animal physiology and behavior remains relatively unexplored.

Like in mammals, tyramine levels in invertebrates are much lower than those of the classic invertebrate biogenic amines, dopamine, serotonin, and octopamine (Monastirioti et al., 1996; Cole et al., 2005; Alkema et al., 2005). In invertebrates, tyramine is also a precursor in the biosynthesis of octopamine, often considered to be the invertebrate analog of norepinephrine (Roeder et al., 2003). In *C. elegans* tyramine is synthesized from tyrosine by a tyrosine decarboxylase (*tdc-1*), and a tyramine β-hydroxylase (*tbh-1*) is required to convert tyramine to octopamine (Alkema et al., 2005). TDC-1 and TBH-1 are coexpressed in a single pair of interneurons, the RICs, and in gonadal sheath cells, indicating that these cells are octopaminergic. TDC-1 is also expressed on its own in the RIM motor neurons and the uterine UV1 cells suggesting that these cells are uniquely tyraminergic in *C. elegans*. Furthermore, animals that lack tyramine and octopamine (*tdc-1* mutants) have behavioral defects that are not shared by animals that only lack octopamine (*tbh-1* mutants), suggesting a distinct role for tyramine in *C. elegans* behavior (Alkema et al., 2005). *tdc-1* mutants, unlike *tbh-1* mutants, have defects in egg laying and reversal behavior and fail to suppress head movements in response to gentle anterior touch. The *C. elegans* neural wiring diagram (White et al., 1986) and cell ablation studies indicate that the tyraminergic RIM motor neurons link the neural circuits that control locomotion and head movements. In the wild, the suppression of head movements in response to touch may allow the animal to escape nematophagous fungi that trap nematodes with constricting hyphal rings (Barron, 1977).

The study of relatively simple circuits in invertebrates has provided fundamental insights on how biogenic amines change the output of distinct motor programs (Marder and Bucher, 2001; Katz et al., 1994; Nusbaum and Beenhakker, 2002). In this report, we show that tyramine inhibits head movements and induces long backward runs through the activation of a tyramine-gated chloride channel, LGC-55. *lgc-55* is expressed in cells that are postsynaptic to the tyraminergic RIM neurons and the activation of LGC-55 inhibits the neural circuits that drive head movements and locomotion. Our data firmly establish tyramine as a classical neurotransmitter in *C. elegans* and suggest that fast inhibitory tyraminergic transmission plays a critical role in coordinating a *C. elegans* escape response.

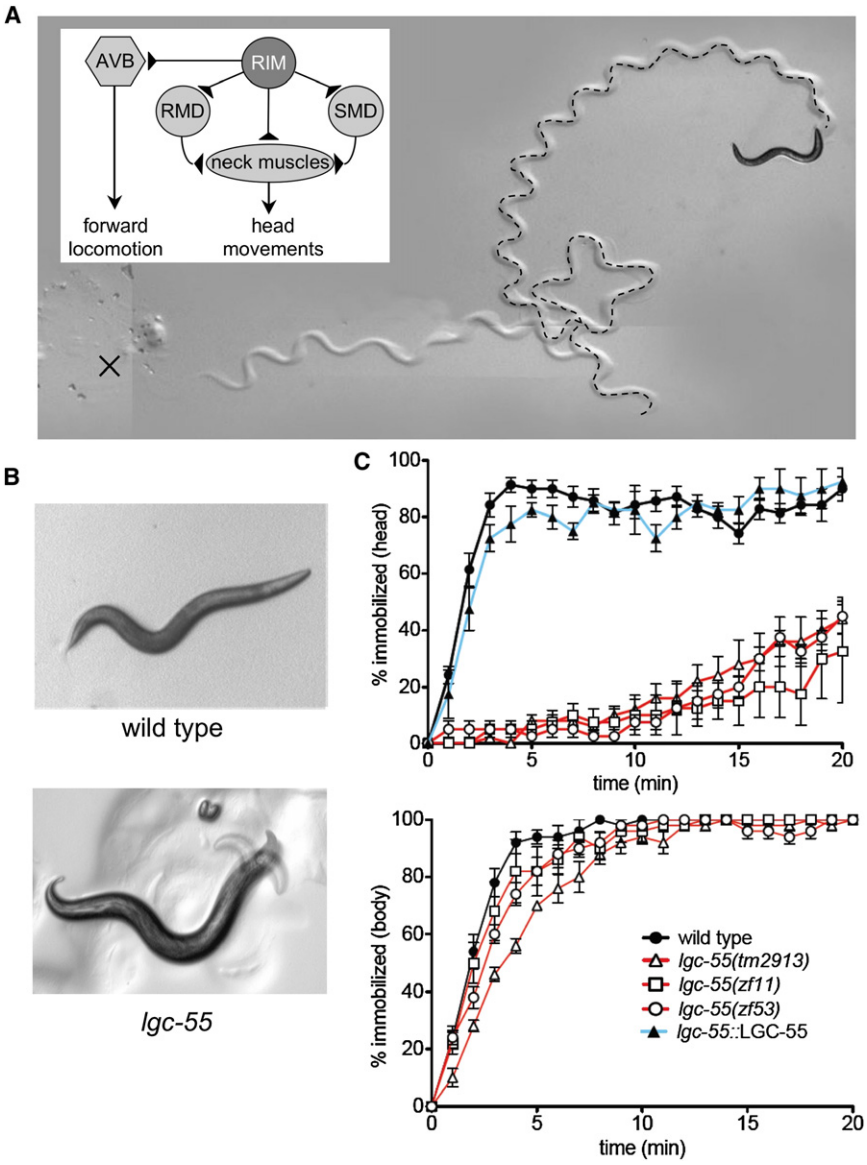

Figure 1. Exogenous Tyramine Induces Long Reversals and Suppresses Head Movements

(A) Still image of locomotion pattern of wild-type animals on 30 mM tyramine prior to immobilization. The x marks the starting location and the dashed line marks the backward locomotory run (see Movie S1). Inset: the main synaptic outputs of the tyraminergic RIM motor neurons include the AVB forward locomotion command neurons, the RMD and SMD motor neurons and neck muscles.

(B) Overlay of three still images of wild-type and *lgc-55(zf11)* after five minutes on exogenous tyramine. Images were taken approximately 2 s apart. Wild-type animals completely immobilize. *lgc-55* mutants move their heads while their body remains immobilized (see Movie S3).

(C) Quantification of head and body movements on 30 mM tyramine. Shown is the percentage of animals immobilized by tyramine each minute for 20 min. Each data point is the mean ± standard error of the mean (SEM) for at least four trials totaling 40 or more animals. *lgc-55* mutants continue to move their heads through the duration of the assay, while the body immobilizes similarly to wild-type animals.

RESULTS

Exogenous Tyramine Induces Backward Locomotion and Inhibits Head Movements

C. elegans moves on its side in a sinusoidal pattern by propagating dorsoventral waves of body wall muscle flexures along the length of its body. Locomotion is accompanied by exploratory head movements, where the tip of the nose of the animal moves from side to side. Head movements are controlled independently from body movements by a set of radially symmetric head and neck muscles. The tyraminergic RIM motor neurons make synaptic connections with neck muscles that control head movements and command neurons that drive locomotion (Figure 1). To study how tyramine signaling might control head and body movements during locomotion, we developed a simple assay for measuring behavioral responses to tyramine. We found that wild-type animals became immobilized on agar plates containing exogenous tyramine in a dose-dependent manner (see Figure S1 available online). In extended behavioral studies of individual worms in the presence of 30 mM exogenous tyramine, we noted a progressive sequence of behaviors that were nearly invariant from animal to animal (Figure 1). Wild-type animals displayed a brief period of forward locomotion in which head movements ceased completely, while sinusoidal body movements in the posterior half of the animal persisted. Immobilization of head movements was followed by strikingly long backward locomotory runs (Figures 1A and 7D; Movie S1). Following this behavioral sequence, most wild-type animals became completely immobilized within 5 min of tyramine exposure. Locomotion could still be triggered in immobilized animals by mechanical stimulation with a platinum wire. However, movements were restricted to the posterior half of the animal (body movements) while the head remained paralyzed (Movie S2). These results support the idea that exogenous tyramine affects head movements and locomotory body movements through distinct tyraminergic signaling pathways.

lgc-55 Mutants Are Partially Resistant to Exogenous Tyramine

To identify genes involved in tyramine signaling we performed a genetic screen for mutants that are resistant to the paralytic

effects of exogenous tyramine. We placed F2 progeny of 10,000 mutagenized hermaphrodites on agar plates containing 30 mM tyramine and selected rare mutants that displayed sustained body and/or head movements. Two mutants isolated from this screen, *zf11* and *zf53*, became immobilized slightly more slowly than wild-type animals and continued head movements on plates containing exogenous tyramine (Figures 1B and 1C). However, neither *zf11* nor *zf53* mutant animals displayed any body movements posterior to the pharynx (Movie S3). Furthermore, exogenous tyramine failed to induce long backward locomotory runs in the *zf11* and *zf53* mutants (Figure 7D). *zf11* and *zf53* mutant animals were healthy and viable with normal brood sizes and had no obvious defects in locomotion pattern or head movements in the absence of exogenous tyramine.

We mapped *zf11* using single nucleotide polymorphisms and three-factor mapping to the right of chromosome V close to *unc-51* (Figure 2A). This genomic region contains a gene, *lgc-55*, which encodes a protein with similarity to members of the cysteine-loop ligand-gated ion channels (Cys-loop LGIC; Figure 2B; Betz, 1990). Sequence analysis revealed single-base transitions in the *lgc-55* coding sequence in *zf11* and *zf53* mutants. The *lgc-55* gene structure was confirmed by analysis of expressed sequence tagged full-length cDNA clones. The predicted LGC-55 protein is comprised of a large extracellular ligand-binding domain with a characteristic Cys-loop motif, four transmembrane domains (M1–M4), and a large intracellular domain between M3 and M4 (Figure 2C). The *zf11* allele mutates a splice acceptor site of exon 9, which causes a frame shift that would lead to premature truncation of the LGC-55 protein. The *zf53* allele converts the first cysteine codon of the Cys-loop to a tyrosine (C215Y). The cysteines of the Cys-loop motif in the N-terminal extracellular ligand-binding region of each subunit form a disulphide bond that plays a key role in receptor assembly (Green and Wanamaker, 1997) and gating of the ion channel (Grutter et al., 2005). We also obtained an available deletion allele *tm2913*, which deletes parts of both exon 4 and 5 of the *lgc-55* gene. The deletion should prematurely truncate the LGC-55 protein and therefore most likely represents a null allele. Like *lgc-55(zf11)* and *lgc-55(zf53)* mutants, *lgc-55(tm2913)* mutants animals are resistant to tyramine-mediated head paralysis, suggesting that *lgc-55(zf11)* and *lgc-55(zf53)* also represent loss-of-function alleles. We were able to restore tyramine sensitivity by expressing a transgenic *lgc-55* minigene in *lgc-55* mutants (Figure 1C). These data indicate that *lgc-55* is required for the paralytic effects of exogenous tyramine on head movements.

LGC-55 Is an Ionotropic Tyramine Receptor

Cys-loop LGIC receptors, like nicotinic acetylcholine (nAChR), γ-aminobutyric acid ($GABA_AR$), glycine (GlyR), and serotonin ($5HT3_AR$) receptors, form pentameric complexes in the cell membrane (Betz, 1990). Ligand binding at the N-terminal domain induces a conformational change causing the pore of the channel to open. LGC-55 is most closely related to this family of ligand-gated ion channels, in particular the GABA-, glycine-gated chloride channels as well as the *C. elegans* 5HT-gated chloride channel, MOD-1 (Ranganathan et al., 2000; Figure 2B). Additionally, we identified orthologs of LGC-55 in the genomes of the closely related nematode species *C. briggsae* (CBP26358, 99% identity), *C. remanei* (RP28082, 99% identity), *Pristionchus pacificus* (PP01401, 70% identity), and the more distantly related parasitic nematode *Brugia malayi* (EDP32880, 52% identity).

To determine whether LGC-55 can form functional homomeric channels, we expressed *lgc-55* in *Xenopus laevis* oocytes for two-electrode voltage clamp recordings. In *lgc-55* injected oocytes, application of tyramine in concentrations ranging from 1–1000 μM evoked robust and rapidly developing inward currents up to 2.2 μA (Figure 3A). Application of tyramine to mock injected oocytes showed no such response (data not shown). The EC_{50} (effective concentration for half maximal response) for tyramine activation of LGC-55 receptors was 12.1 ± 1.2 μM, a concentration well within the range of EC_{50} values defined for neurotransmitters that activate closely related LGIC family members (Figure 3B). These data indicate that LGC-55 forms a functional homomeric receptor that can be activated by tyramine. The EC_{50} of the structurally related amines, octopamine and dopamine, is approximately 10-fold lower than those for tyramine (EC_{50} = 215.2 ± 1.1 μM and 158.8 ± 1.1 μM respectively), whereas serotonin only elicited small LGC-55-dependent inward currents at millimolar concentrations. GABA, glycine, acetylcholine, and histamine did not elicit any significant LGC-55-dependent inward currents even at concentrations as high as 1 mM. Although octopamine and dopamine may activate LGC-55 in vivo, tyramine is the most potent activator of LGC-55, suggesting that tyramine could function as the native ligand for LGC-55.

LGC-55 Is a Tyramine-Gated Chloride Channel

The ion selectivity of cys-loop LGICs is determined by the M2 domain, which lines the pore of the ion channel. LGC-55 contains a PAR motif on the cytoplasmic side of the M2 domain, which is conserved in most anion-selective channels (Figure 3D; Karlin and Akabas, 1995). To determine the ion selectivity, we analyzed the current-voltage (*I-V*) relationship for LGC-55 under a variety of ionic conditions. Under our standard recording conditions (100 mM Cl^-), current responses to tyramine application reversed at −25.7 ± 0.9 mV (Figure 3C), consistent with the chloride equilibrium potential (E_{Cl}) in *Xenopus* oocytes (Weber, 1999). This is similar to the reported reversal potential of other *C. elegans* chloride selective channels, such as the UNC-49B/GABA receptor (Bamber et al., 1999) and the serotonin-gated chloride channel, MOD-1 (Ranganathan et al., 2000) and significantly different from the near 0 mV reversal potential normally observed for nonselective cation channels. Furthermore, after complete substitution of extracellular sodium with the large impermeant cation *N*-methyl-D-glucamine (NMDG), we did not observe an obvious change in reversal potential (E_{rev}NMDG = −27.2 ± 1.3 mV), suggesting that sodium ions do not significantly contribute to the current passing through the LGC-55 ion channel (Figure 3C).

To test how changes in the chloride ion concentration affected the reversal potential of LGC-55, we substituted external chloride with the large anion gluconate. When the chloride concentration was reduced by 10-fold, we observed a rightward shift in reversal potential of approximately 40 mV (E_{rev}gluconate = 14.9 ± 2.6; Figure 3C). These data are

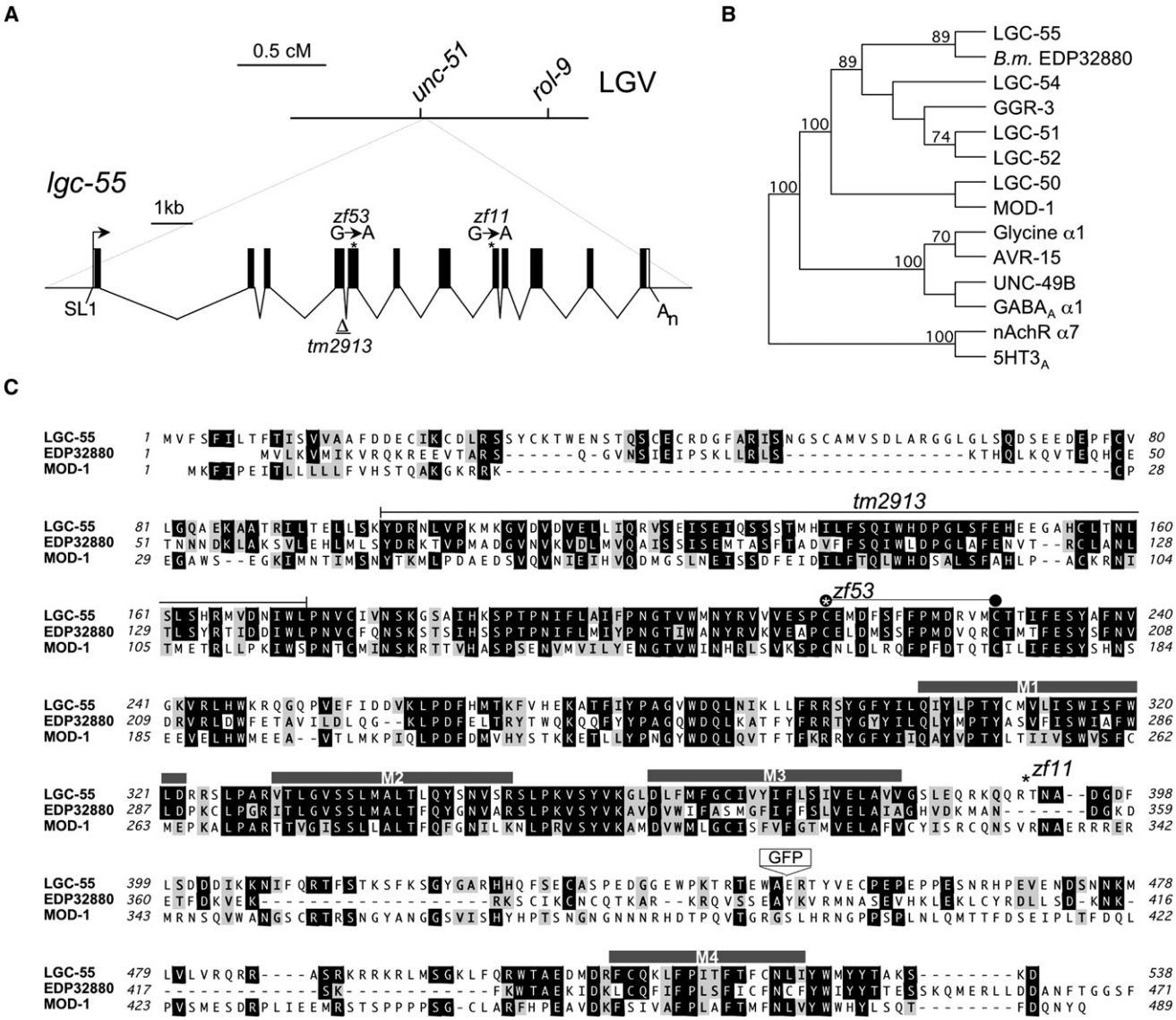

Figure 2. *lgc-55* Encodes a Ligand-Gated Ion Channel Subunit

(A) The *lgc-55* locus. Genetic map and gene structure of *lgc-55*: coding sequences are represented as black boxes; untranslated regions are represented as white boxes. The SL1 *trans*-spliced leader and the poly(A) tail are indicated. The position of the *lgc-55(zf11)* allele *lgc-55(zf53)* and *lgc-55(tm2193)* allele are indicated. The *lgc-55(tm2913)* has a 285 bp deletion that removes part of exon 4 and exon 5. The deleted region indicated by bars.

(B) Phylogenetic tree of LGC-55 and various ligand-gated ion channel subunits. Predicted *C. elegans* LGICs (Jones and Sattelle, 2008), including the 5HT receptor MOD-1, glutamate receptor AVR-15, GABA receptor UNC-49$_B$, the *Brugia malayi* predicted protein EDP32880, and human GABA$_A\alpha$1, nAchRα7 and 5HT3$_A$. A neighbor weighted tree of decarboxylase-conserved regions based on bootstrap analysis and the Unweighted pair group method with arithmetic mean (UPGMA) was determined using MacVector software (Accelrys).

(C) Alignment of LGC-55 with MOD-1 and the closely related predicted protein from *Brugia malayi*, EDP32880. Identities are outlined in black and similarities are shaded. The four predicted transmembrane domains are indicated by black bars, and the Cys-loop is indicated by a line with two black with black circles. The LGC-55 *zf11* and *zf53* mutations are indicated by stars, the black line denotes the amino acids deleted in the *tm2913* allele. The position of the GFP insertion of the LGC-55::GFP translational fusion is indicated.

consistent with corresponding shifts predicted by the Nernst equation and indicate that LGC-55 is a chloride selective channel. To test whether the LGC-55 receptors expressed in vivo were also chloride selective, we expressed *lgc-55* in *C. elegans* body wall muscles using the muscle-specific *myo-3* promoter (*myo-3::* LGC-55) and recorded current responses to tyramine using whole-cell patch clamp electrophysiology (Figure 3E). While we never detected measurable current responses to tyramine in body wall muscles of wild-type worms, we noted robust responses to tyramine in the body wall muscles of transgenic worms expressing LGC-55. Consistent with our results for heterologously expressed LGC-55 receptors, current responses to

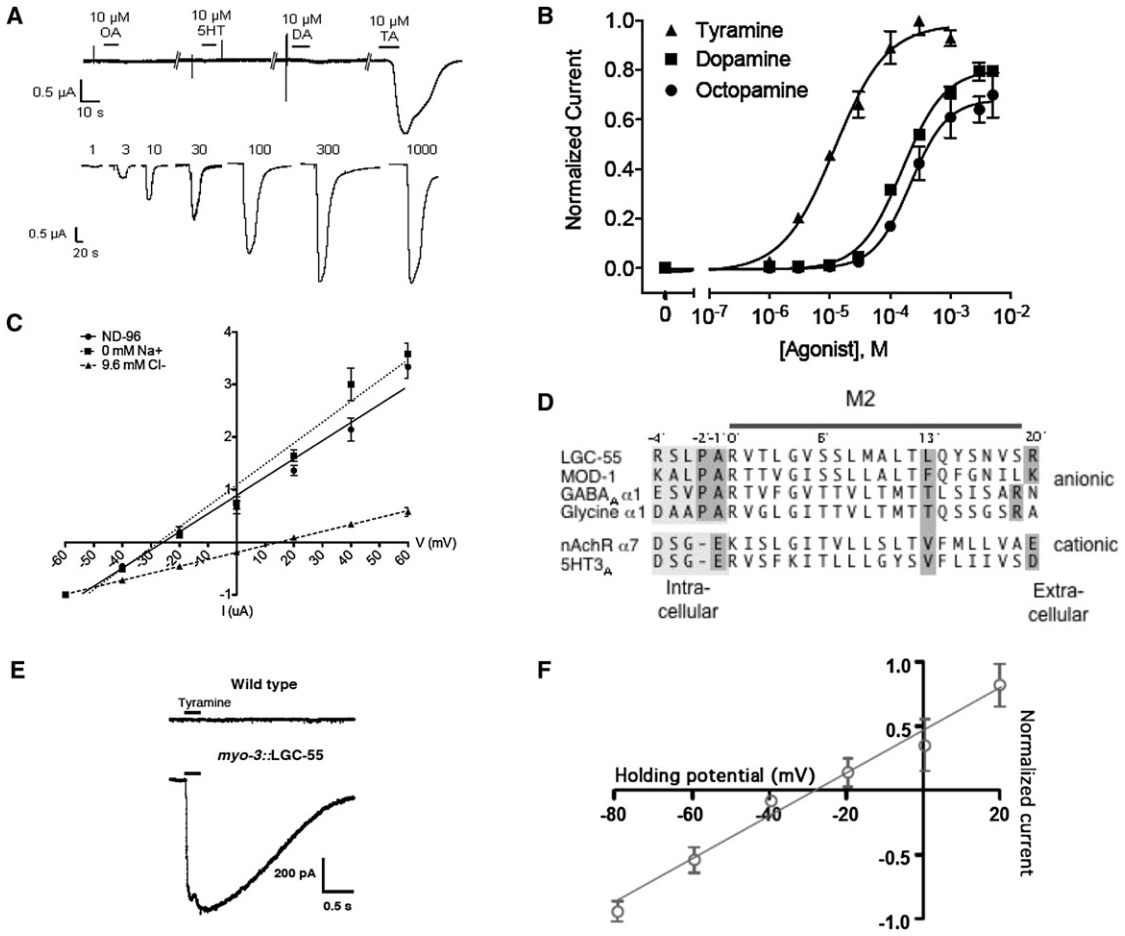

Figure 3. LGC-55 Is a Tyramine Gated Chloride Channel

(A) Representative traces from *Xenopus* oocytes injected with *lgc-55* cRNA showing responses to 10 μM octopamine (OA), serotonin (5HT), dopamine (DA), and tyramine (TA) as well 1–1000 μM TA in ND-96. Neurotransmitters were bath applied for 10 s.

(B) LGC-55 TA, OA and DA dose response curves. EC_{50}TA = 12.1 ± 1.2 μM and Hill coefficient = 1.0 ± 0.17, EC_{50}DA = 158.8 ± 1.1 μM, EC_{50}OA = 215.2 ± 1.1 μM. Each data point represents the mean current value normalized to the mean maximum current observed for tyramine, (I_{max} = 2.2 ± 0.17 μA). Error bars represent SEM.

(C) Ion selectivity of LGC-55 in *Xenopus* oocytes. TA-evoked (10 μM, 10 s) currents were recorded at the holding potentials shown. Circles: standard ND-96 (E_{rev} = −25.7 ± 0.9 mV, n = 4); squares: 0 mM Na^+ (E_{rev} = −27.2 ± 1.3 mV, n = 4); triangles: 9.6 mM Cl^- (E_{rev} = 15.0 ± 2.6 mV, n = 4). *I-V* curves were plotted using linear regression, error bars represent SEM.

(D) Alignment of the M2 region of LGC-55 with other members of the Cys-loop ligand-gated ion channel family. Shaded regions indicate residues important for ion selectivity.

(E) Representative current responses to tyramine application (200 μM) recorded from *C. elegans* body wall muscle cells of wild-type (upper) or transgenic animals expressing *myo-3*::LGC-55 (lower). Black bars indicate duration of tyramine application (250 ms).

(F) Current-voltage relationship for LGC-55 receptors expressed in *C. elegans* body wall muscle cells under normal recording conditions. Current responses to tyramine were recorded at the holding potentials indicated.

tyramine reversed at approximately –30 mV (Figure 3F), near the predicted reversal potential for an anion-selective channel under our conditions (Francis and Maricq, 2006).

LGC-55 Is Expressed in Cells that Are Postsynaptic to the Tyraminergic RIM Motor Neurons

To determine the expression pattern of *lgc-55* we generated translational fluorescent reporter constructs. A 7 kb *lgc-55* genomic fragment including a 3.5 kb promoter and the first intron was fused to the open reading frame of green (GFP) (Chalfie et al., 1994) and red (mCherry) fluorescent reporters (Shaner et al., 2004). *lgc-55*::mCherry and *lgc-55*::GFP transgenic animals showed reporter expression in a subset of neck muscles and a restricted set of neurons (Figure 4). We have identified these neurons as the AVB, RMD, SMDD, SMDV, IL1D, IL1V, SDQ, HSN, and ALN neurons (Figures 4A, 4B, 4C, and S2–S4). In addition, weak *lgc-55* reporter expression was also detected in the UV1 cells and tail muscle cells.

To visualize the localization of the LGC-55 protein we fused the GFP coding sequence between the M3 and M4 coding domain

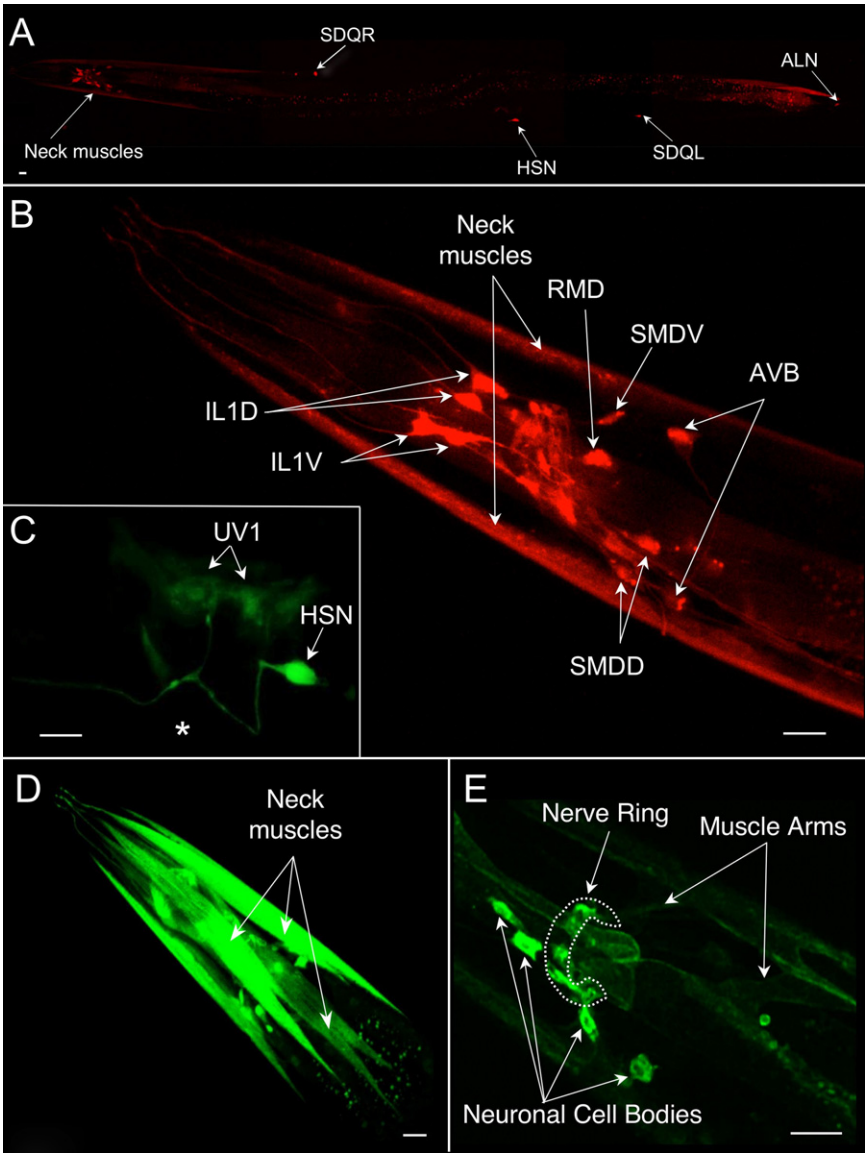

Figure 4. Expression Pattern of *lgc-55*

(A) Adult animal showing expression of a fluorescent *lgc-55*::mCherry (*zfIs4*) transcriptional reporter in neck muscles, head neurons, SDQ, HSN, and ALN neurons.

(B) Head region of an adult animal showing expression of *lgc-55*::mCherry in head neurons, IL1, RMD, SMD, and AVB.

(C) Expression of *lgc-55*::GFP (*zfIs6*) in the HSN and uterine UV1 cells. The star indicates position of the vulva.

(D) Expression of *lgc-55*::GFP in the third row of neck muscle cells.

(E) Expression of LGC-55::GFP (*zfEx38*) translational reporter showing subcellular localization to neuronal cell bodies, nerve ring and muscle arms. Position of the nerve ring is indicated by the dotted line. Scale bar, 10 μm. Anterior is to the left and ventral side is down in all images.

of the minimal rescuing construct. The LGC-55::GFP construct rescued the sensitivity of *lgc-55(tm2913)* mutants to exogenous tyramine and also rescued defects in the suppression of head oscillations (data not shown), indicating that LGC-55::GFP is, at least in part, properly localized to restore tyraminergic signaling. LGC-55::GFP fluorescence was observed in neuronal cell bodies and punctate structures in the nerve ring, suggestive of postsynaptic specializations (Figure 4E). In *C. elegans*, muscles extend cytoplasmic arms that synapse with bundles of motor neuron processes (White et al., 1986; Hall and Altun, 2007). Neck muscle arms turn anteriorly into the nerve ring where they make synapses with the head motor neurons including the tyraminergic RIMs. Therefore, the LGC-55::GFP puncta in the nerve ring suggest that LGC-55 receptors cluster at post synaptic sites that may include neuromuscular synapses between the RIMs and the neck muscles. The neck muscles, the AVB, RMD, SMDD, and SMDV neurons are postsynaptic to the tyraminergic RIM motor neurons (White et al., 1986), consistent with tyramine being an endogenous ligand of LGC-55. The HSN, IL1, SDQ, and ALN neurons send processes to the nerve ring but do not receive direct synaptic input from the RIM, suggesting that LGC-55 may also act extrasynaptically. Furthermore, tyramine release from non-neuronal cells, such as the uterine UV1 cells, could activate LGC-55.

lgc-55 Is Required in Neck Muscles to Suppress Head Oscillation in Response to Anterior Touch

Gentle touch to the anterior half of the body of *C. elegans* elicits an escape response in which the animal reverses its direction of locomotion (Chalfie et al., 1985). Wild-type animals suppress head oscillations during this backing response (Movie S4). Mutant animals that lack tyramine, and animals in which the tyraminergic RIM motor neurons are ablated fail to suppress head oscillations in response to anterior touch (Alkema et al., 2005). *lgc-55* mutants had no obvious defects in locomotion pattern or head oscillations during normal foraging. However, we found that *lgc-55* mutant animals failed to suppress head oscillations in response to anterior touch (Figure 5; Movie S5).

How does the tyramine-gated chloride channel suppress head oscillations in response to anterior touch? Head movements that accompany foraging behavior are controlled by the excitatory cholinergic RMD and SMD neurons and the inhibitory GABAergic RME neurons that provide synaptic inputs to the neck muscles (Hart et al., 1995; Gray et al., 2005). The RMD and SMD neurons are coupled through gap junctions and reciprocal synaptic connections, and innervate contralateral neck muscles (White et al., 1986). The RMD neurons display bistable

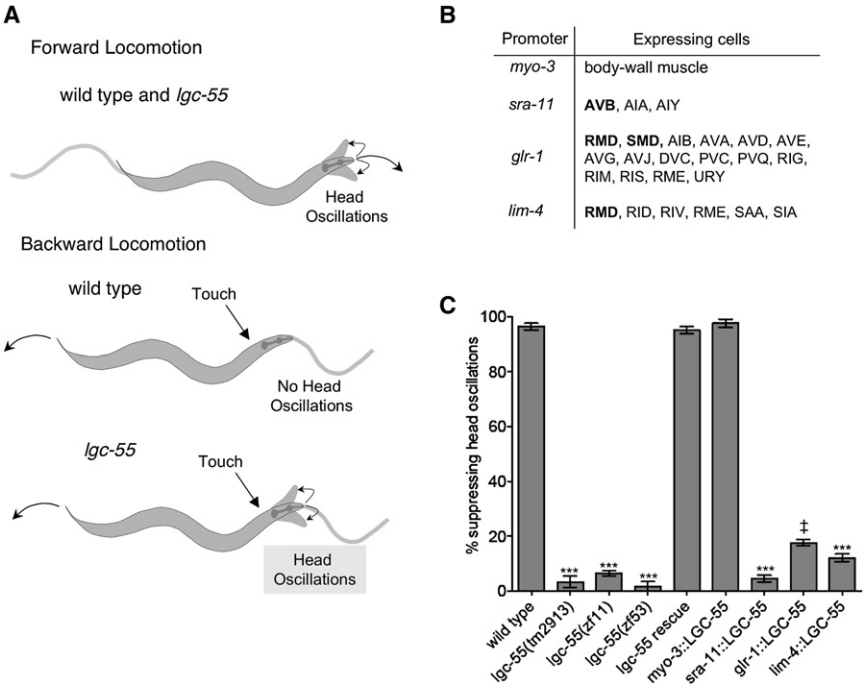

Figure 5. *lgc-55* Mutants Fail to Suppress Head Oscillations in Response to Anterior Touch

(A) Illustration of *C. elegans* head movements during locomotion. Wild-type animals and *lgc-55* mutants oscillate their heads during forward locomotion. Anterior touch of wild-type animals with an eyelash induces a reversal response during which the head oscillations are suppressed. *lgc-55* mutants fail to suppress head oscillations during the reversal.

(B) Expression patterns of promoters used for cell-specific rescue of *lgc-55*: *lim-4* (Sagasti et al., 1999); *glr-1* (Hart et al., 1995; Maricq et al., 1995); *sra-11* (Altun-Gultekin et al., 2001); and *myo-3* (Okkema et al., 1993). Note: We could not detect expression of a *glr-1*::GFP reporter in the AVB neurons of adult transgenic animals; See Figures S2–S4. Cells overlapping with *lgc-55* expression are indicated in bold.

(C) Suppression of head oscillations in response to anterior touch was scored during the reversal response, wild-type (n = 235), *lgc-55* mutants (*lgc-55(tm2913)* [n = 205], *lgc-55(zf11)* [n = 205], *lgc-55(zf53)* [n = 170]), *lgc-55* rescue (*lgc-55 (tm2913); zfEx2* [n = 205]), *myo-3*::LGC-55 (*lgc-55(tm2913); zfEx31* [n = 100]), *sra-11*::LGC-55 (*lgc-55(tm2913); zfEx37* [n = 185]), *glr-1*::LGC-55 (*lgc-55(tm2913); zfEx42* [n = 130]), and *lim-4*::LGC-55 (*lgc-55(tm2913); zfEx44* [n = 115]) . Error bars represent SEM. Statistical difference from wild-type; ***p < 0.0001, two-tailed Student's t test. ‡p < 0.0001, two- tailed Student's t test. *glr-1*::LGC-55 transgenic animals do not completely suppress head oscillations and appear to have a kinked head during reversals in response to anterior touch. See text for details.

potentials, which may contribute to the oscillatory head movements (Mellem et al., 2008). The GABAergic RME neurons synapse onto the neck muscles as well as the RMD and SMD neurons and limit the extent of head deflection during head oscillations (McIntire et al., 1993).

We observed strong *lgc-55*::GFP expression in the RMD and SMD neurons as well as eight radially symmetric neck muscle cells (Figures 4B and 4D). We therefore sought to identify the cells in which *lgc-55* acts to suppress head oscillations in response to anterior touch using cell specific rescue and mosaic analysis. For the first approach, we expressed the *lgc-55* cDNA under the control of cell specific promoters in the *lgc-55(tm2913)* mutants. We used the following promoters to drive the expression of *lgc-55* in specific subsets of cells: *lim-4*: the RMD neurons (plus 5 additional neurons; Sagasti et al., 1999); *glr-1:* the RMD and SMD neurons (plus 14 additional neurons; Hart et al., 1995; Maricq et al., 1995); *sra-11*: the AVB neurons (plus 2 additional neurons; Altun-Gultekin et al., 2001) and *myo-3*: body wall muscle (including neck muscle; Okkema et al., 1993; Figure 5B). Expression of *lgc-55* in the AVB (*sra-11::*LGC-55) or RMD (*lim-4::*LGC-55) neurons failed to rescue the defect in the suppression of head oscillations (Figure 5C). Animals that expressed *lgc-55* in the RMD and SMD neurons (*glr-1::*LGC-55) also did not fully rescue the suppression of head oscillations but usually kinked their head to one side while reversing. However, RMD and SMD expression did restore sensitivity to the paralyzing effects of exogenous tyramine in head movement assays (Figure S5). The expression of *myo-3::*LGC-55 in muscle, on the other hand, fully rescued the defect in the suppression of head oscillations of *lgc-55* mutants (Figure 5C) and restored sensitivity to the paralyzing effects of exogenous tyramine in head movement assays (Figure S5). Animals in which *lgc-55* expression was rescued in body wall muscle displayed normal locomotion and backing in response to touch, suggesting that tyraminergic activation of *lgc-55* mainly occurred synaptically at the RIM-neck muscle neuromuscular junctions.

As a second approach, we performed genetic mosaic analysis. The *lgc-55* expressing neurons are derived from the embryonic AB blastomere, whereas the body wall muscles are derived from the P1 blastomere (Figure 6A). Using GFP and mCherry markers, we selected animals that had lost a rescuing extrachromosomal array in either the descendants of the AB blastomere or the descendants of the P1 blastomere. Mosaic animals that lost the array in the P1 lineage failed to suppress head oscillations whereas animals that lost the array in the AB lineage did suppress head oscillations in response to touch (Figure 6B). Exogenous tyramine could still inhibit head movements in animals that lost the rescuing array in the P1 lineage, albeit to lesser extent than animals that lost the array in the AB lineage. These results indicate that even though LGC-55 expression in the RMD and SMD neurons may contribute to the suppression, LGC-55 expression in neck muscles is necessary and sufficient to fully suppress lateral head movements upon anterior touch. However, *lgc-55* expression in neurons was required to mediate the tyraminergic stimulation of backward locomotion, since exogenous tyramine did not induce long backward locomotory

A

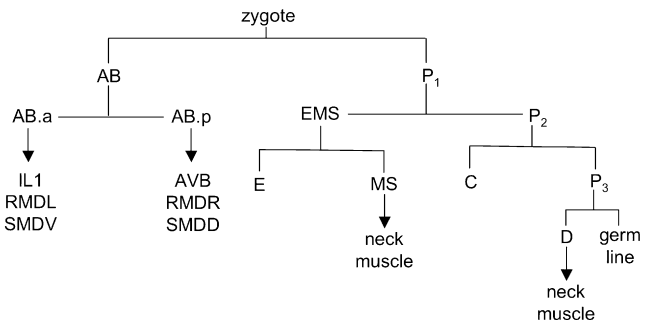

B

Expressing Cells	n	% supp. head oscillations	% head paralysis	longest backward run
All	11	100	100	26 +/- 3.5
None	13	0	0	1.8 +/- 0.3
Muscle	7	97 +/- 2.8	100	1.7 +/- 0.5
Neurons	6	17 +/- 3.3	67 +/- 21	14 +/- 5.1

Figure 6. *lgc-55* Is Required in Neck Muscles to Suppress Head Oscillations

(A) Diagram of *C. elegans* early cell lineage. *lgc-55* expressing cells derived from AB and P1 are indicated.

(B) Mosaic analysis. An *lgc-55* rescuing construct was injected into *lgc-55(tm2913)* mutant animals together with *lgc-55::*mCherry and *myo-3*::GFP as lineage markers. Animals lacking *lgc-55* function in either the AB or P1 lineages and nonmosaic controls were analyzed for suppression of head oscillations in response to anterior touch, head paralysis after 5 min. on exogenous tyramine (30 mM) and longest backward run on 30 mM tyramine. Data shown are the mean ± SEM.

runs in animals that had lost the array in the AB lineage (see below).

lgc-55 Acts in the AVB Forward Locomotion Command Neurons to Modulate Reversal Behavior

On agar plates *C. elegans* mainly displays forward locomotion interrupted by brief backward locomotory runs. The neural circuit that controls forward and backward locomotion consists of four pairs of locomotion command interneurons: the PVC and AVB neurons are primarily required for forward locomotion whereas the AVD and AVA neurons are required for backward locomotion (Chalfie et al., 1985). Electrophysiology, Ca^{2+} imaging and genetic experiments indicate that depolarization of the forward locomotion command neurons results in forward locomotion whereas depolarization of the backward locomotion command neurons drives backward locomotion (Chronis et al., 2007; Zheng et al., 1999). The forward and backward locomotion command neurons make reciprocal synaptic connections, which may link the neural activities underlying these antagonistic behaviors and allow the animal to switch its direction of locomotion. The tyraminergic RIM neurons are electrically coupled through gap junctions with the AVA backward command neurons and have synaptic outputs onto the AVB forward locomotion command neurons. Although tyramine deficient animals normally initiate backward locomotion in response to anterior touch, they back up less far than the wild-type. In addition, tyramine deficient animals have a marked increase in the number of spontaneous reversals indicating that tyramine modulates reversal behavior (Alkema et al., 2005).

We tested whether *lgc-55* mutants have defects in reversal behavior. Like *tdc-1* mutants, *lgc-55* mutants initiated backward locomotion normally in response to anterior touch but displayed shorter runs of backward movement (2.4 ± 0.1 body bends) than the wild-type (3.3 ± 0.1 body bends) (Figures 7A and S6). In addition, we found that *lgc-55* mutants had an increase in spontaneous reversals compared to the wild-type, although the increase was less pronounced than that of the *tdc-1* mutants (Figure 7B). To examine spontaneous reversal behavior in more detail we categorized the reversals according to the number of backward body bends (Gray et al., 2005). We found that *lgc-55* mutants displayed more short reversals than wild-type worms (Figure 7C). The increase in short reversals was even more dramatic in the *tdc-1* mutants. An *lgc-55* minigene rescued the defects of *lgc-55* mutants in reversal behavior in both the touch-induced and spontaneous reversal assays.

Where does *lgc-55* act to increase the length of reversals? Cell specific rescue experiments showed that *lgc-55* expression in the RMD (*lim-4::LGC-55*), RMD or SMD neurons (*glr-1::LGC-55*) or body wall muscle (*myo-3::LGC-55*) did not restore normal reversal behavior in *lgc-55* mutants (Figure 7A, data not shown). However, *lgc-55* expression in the AVB neurons (*sra-11::LGC-55*) restored normal reversal behavior in *lgc-55* mutants. The length of backward runs in response to anterior touch (on average 3.3 ± 0.2 backward body bends), and the number and percentage of long reversals (39.6% short versus 60.4% long) in spontaneous reversal assays were comparable to those observed for wild-type worms (Figure 7). These data indicate that *lgc-55* expression in the AVB neurons is required to sustain backward locomotion once a reversal is initiated.

Our data support the hypothesis that tyramine inhibits forward locomotion by activating *lgc-55* and hyperpolarizing the AVB forward locomotion command neurons. The *lgc-55* dependent inhibition of the forward locomotion program could dramatically shift the balance toward the backward locomotion program, thus explaining our observation that exogenous tyramine induces extremely long backward locomotory runs. To further test this hypothesis, we quantified reversal behavior in the presence of exogenous tyramine. The longest average backward run for wild-type worms in the presence of exogenous tyramine was approximately 15 body bends, compared to 4 body bends in the absence of exogenous tyramine (Figure 7D). However, exogenous tyramine did not elicit prolonged backward runs in *lgc-55* mutant animals (4.0 versus 2.8 backward body bends, respectively). In contrast, *lgc-55* mutants that carried a rescuing *lgc-55* transgene displayed a dramatic increase in the length of backward runs in this assay (44 backward body bends), likely due to overexpression of *lgc-55*. Exogenous tyramine also triggered long backward runs (11 backward body bends) in *lgc-55* mutants that express *lgc-55* in the AVB neurons using the *sra-11*::*lgc-55* transgene (Figure 7D) but failed to do so in animals that express *lgc-55* in the SMD and/or RMD neurons or body

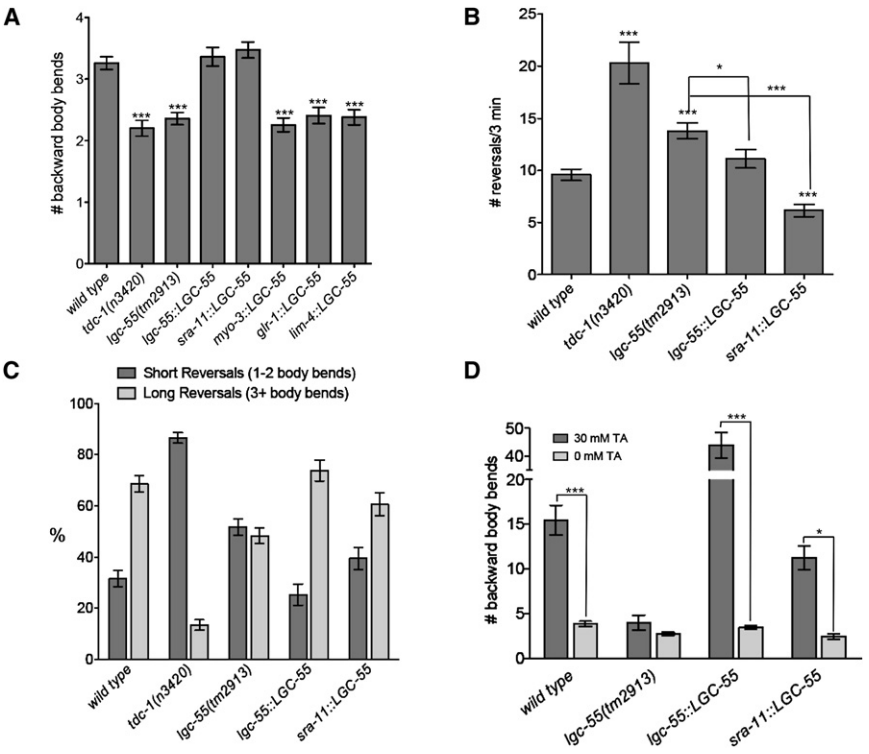

Figure 7. *lgc-55* Mutants Have Defects in Reversal Behavior

(A) Average number of backward body bends in response to anterior touch of wild-type (n = 317), *tdc-1(n3420)* (n = 139), *lgc-55(tm2913)* (n = 257), *lgc-55* rescue (*lgc-55(tm2913); zfEx2* [n = 204]), *sra-11*::LGC-55 (*lgc-55(tm2913); zfEx37* [n = 190]), *myo-3*::LGC-55 (*lgc-55(tm2913); zfEx31* [n = 157]), *glr-1*::LGC-55 (*lgc-55(tm2913); zfEx42* [n = 133]), and *lim-4*::LGC-55 (*lgc-55(tm2913); zfEx44* [n = 108]) animals.

(B) Number of spontaneous reversals in 3 min of well fed wild-type (n = 55), *tdc-1(n3420)* (n = 16), *lgc-55(tm2913)* (n = 40), *lgc-55* rescue (*lgc-55(tm2913); zfEx2* [n = 27]), and *sra-11*::LGC-55 (*lgc-55(tm2913); zfEx37* [n = 32]) animals on plates without food. Statistical difference from wild-type unless otherwise noted; ***p < 0.0001, *p < 0.01, two-tailed Student's t test.

(C) Distribution of short (1–2 body bends) and long (3+ body bends) spontaneous reversals made in 3 min. p < 0.001, two-way ANOVA.

(D) Number of backward body bends made during the longest backward run before paralysis on 30 mM tyramine of wild-type (n = 33), *lgc-55 (tm2913)* (n = 20), *lgc-55* rescue (*lgc-55(tm2913); zfEx2* [n = 20]), and *sra-11*::LGC-55 (*lgc-55 (tm2913); zfEx37* [n = 29]) animals. 0 mM data represent the number of backward body bends during the longest backward run made in 3 min on agar plates without food for wild-type (n = 28), *lgc-55(tm2913)* (n = 20), *lgc-55* rescue (*lgc-55(tm2913); zfEx2* [n = 20]), and *sra-11*::LGC-55 (*lgc-55(tm2913); zfEx37* [n = 12]) animals. p < 0.0001, two-way ANOVA; ***p < 0.001, *p < 0.01, Bonferroni posttest. Error bars represent SEM.

wall muscles (data not shown). This result indicates that the effects of exogenous tyramine on backward locomotion are mediated, at least in part, through the activation of *lgc-55* in the AVB forward locomotion neurons.

DISCUSSION

Tyramine Acts as a Classical Neurotransmitter in *C. elegans*

Although tyramine is found in nervous systems from worms to man, it has remained unclear whether tyramine can act as a bona fide neurotransmitter. The data presented further satisfy the six criteria that tyramine must meet to enter the realm of neurotransmitters (Paton, 1958; Cowan et al., 2001): (1) the presynaptic neuron contains enzymes to make the substance; (2) the substance is released upon activation of the neuron; (3) exogenous application of the substance to the postsynaptic cell mimics normal synaptic transmission; (4) the postsynaptic cell has receptors for the substance; (5) blocking the receptor disrupts the activity of the substance; (6) there are mechanisms to terminate the action of the substance. First, it was previously shown that the *C. elegans* RIM neurons contain the TDC-1 enzyme that synthesizes tyramine. Second, behavioral analysis of *tdc-1* mutants, vesicular monoamine transporter (*cat-1*) mutants and laser ablation studies indicate that activation of the RIM motor neuron leads to synaptic tyramine release (Alkema et al., 2005). Third, here we show that exogenous tyramine, like endogenous tyramine release, leads to the suppression of head oscillations and stimulates backward locomotion. Fourth, cells that are postsynaptic to the RIM express the tyramine-gated chloride channel, LGC-55. Fifth, genetic disruption of the receptor blocks the tyramine-induced suppression of head oscillations and stimulation of backward locomotion. Sixth, to date no tyramine or octopamine reuptake transporter has been characterized in *C. elegans.* However, several of the *C. elegans* sodium neurotransmitter transporter gene family (SNF) (Mullen et al., 2006) have not been characterized. In addition, monoamine-oxidase (MAO) and aryl-alkylamine N-acetyltransferase activities have been detected in nematodes including *C. elegans* (Isaac et al., 1996) indicating that mechanisms that could terminate tyramine action are present in *C. elegans*.

Metabotropic tyramine receptors have been identified in a wide variety of animals. Three G protein-coupled receptors that are activated by tyramine, SER-2, TYRA-2, and TYRA-3, have been identified in *C. elegans* (Rex et al., 2005; Rex and Komuniecki, 2002; Wragg et al., 2007; Tsalik et al., 2003). *ser-2*, *tyra-2*, and *tyra-3*, are expressed in cells that do not receive direct input from the tyraminergic RIMs suggesting that tyramine mainly acts as a neurohormone to activate G protein-coupled tyramine receptors. *ser-2*, *tyra-2*, and *tyra-3* mutants have no obvious defects in the suppression of head oscillations or reversal behavior. However, *ser-2* mutants are partially resistant to the inhibitory effects of tyramine on body movements (J.L.D. and M.J.A, unpublished observations). LGC-55 provides the first example of an ionotropic-tyramine receptor. Ligand-gated ion channels are thought to have arisen from a common ancestor

over 2 billion years ago (Ortells and Lunt, 1995). LGC-55 is found in the same clade as the serotonin-gated chloride channel MOD-1, suggesting that an ancestral anion-channel accumulated mutations in its extracellular domain to acquire sensitivity to tyramine. Have tyramine-gated chloride channels evolved in species other than nematodes? Some observations seem to support this idea. Tyramine increases chloride conductance in the *Drosophila* Malpighian (renal) tubules (Blumenthal, 2005). Furthermore in rats, tyramine induces strong inhibitory effects on the firing rate of caudate and cortical neurons (Henwood et al., 1979) and can induce hyperpolarization in neurons of the subthalamic nucleus (Zhu et al., 2007) of the rat brain.

Tyramine Coordinates Distinct Motor Programs in a *C. elegans* Escape Response

The analysis of escape responses in flies, crayfish and goldfish have illuminated how neural networks translate sensory input into a motor output (Korn and Faber, 2005; Edwards et al., 2002; Allen et al., 2006). An animal's escape response increases its ability to survive predator-prey encounters. One of the main predators of nematodes are the nematophagous fungi (Barron, 1977). These carnivorous fungi are ubiquitous in the soil and decaying organic material and have developed distinctive trapping devices, including constricting hyphal rings, to catch worms (Thorn and Barron, 1984). When a nematode passes through a hyphal ring, gentle friction induces the cells of the ring to inflate and catch the nematode. In *C. elegans* gentle anterior touch is detected by the ALM and AVM mechanosensory neurons (Figure 8; Chalfie and Sulston, 1981). The neural wiring diagram and laser ablation studies support a model by which activation of the ALM and AVM neurons leads to the inhibition of the PVC and AVB forward locomotion command neurons and activation of the AVD and AVA backward locomotion command neurons. This causes the animal to move backward away from the stimulus (Chalfie et al., 1985). Subsequently, the RIM is activated through gap junctions with the AVA neurons triggering the release of tyramine (Alkema et al., 2005) and the activation of tyramine-gated chloride channel, LGC-55.

In response to anterior touch, *lgc-55* mutants, like tyramine deficient animals, fail to suppress head movements and back up less far than the wild-type. This indicates that tyramine modulates the output of two independent motor programs, head movements, and locomotion. *lgc-55* is expressed in neck muscles, the RMD and SMD motor neurons, and the AVB forward locomotion command neurons that receive postsynaptic inputs from the RIM. Our studies indicate that tyramine hyperpolarizes neck muscles through activation of LGC-55, thus relaxing the muscle and inhibiting head movements. Since *lgc-55* is also expressed in the cholinergic RMD and SMD motor neurons, which regulate head movements, hyperpolarization of these motor neurons may further contribute to the inhibition of head movements. Interestingly, recent patch-clamp studies have demonstrated that the RMD neurons display bistable potentials that depend on extrinsic activation of membrane conductance in the RMD neurons (Mellem et al., 2008). The expression of LGC-55 in RMD neurons suggests that tyraminergic inhibitory synaptic input may be important for the generation of RMD bistability.

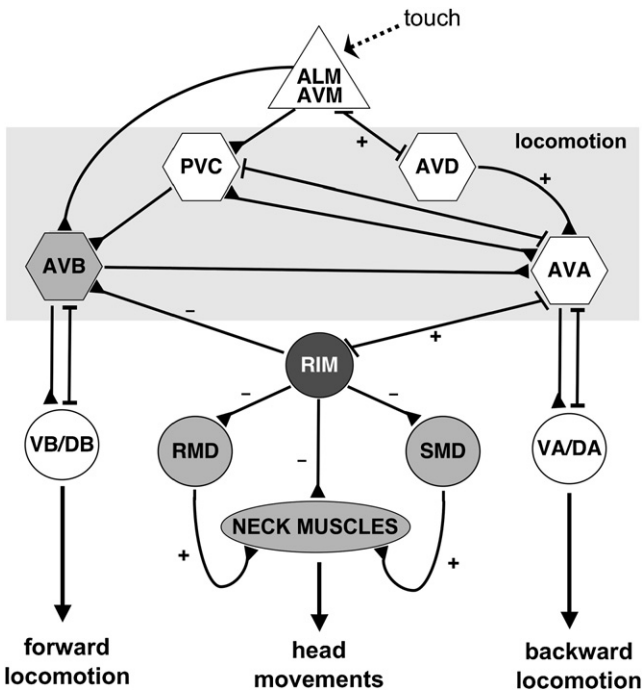

Figure 8. Model: Neural Circuit for Tyraminergic Coordination of *C. elegans* Escape Response

Tyraminergic activation of LGC-55 hyperpolarizes neck muscles and the AVB command neurons inducing suppression of head oscillations and sustained backward locomotion in response to touch. Schematic representation of the neural circuit that controls locomotion and head movements. Synaptic connections (triangles) and gap junctions (bars) are as described by White et al. (1986). Sensory neurons shown as triangles, command neurons required for locomotion are shown as hexagons, and motor neurons are depicted as circles. Neck muscles are represented as an oval. *lgc-55* expressing cells and neurons are light gray. The tyraminergic motor neuron (RIM) is dark gray. Hypothesized excitatory (+) connections of neurons in this circuit are based on the identification of neurotransmitters, laser ablation, and genetic studies cited in this paper. Inhibitory (–) connections important for suppression of head oscillations in response to anterior touch and sustained backward locomotion are based on behavioral, electrophysiological, and expression data described in this paper. See text for details.

LGC-55 expression in the AVB forward locomotion command neurons is required for tyraminergic modulation of reversal behavior. The forward locomotion command neurons make presumptive inhibitory inputs onto the backward locomotion command neurons to coordinate the animal's locomotion program. Our data indicate that tyraminergic activation of LGC-55 in the AVB shifts the balance of the bistable circuit that controls the direction of locomotion in favor of the backward locomotion program. Tyramine reinforces the backward locomotion program allowing the animal to make a long reversal before reinitiating forward locomotion (Figure 8). Long reversals (three or more body bends) are usually coupled to an omega turn, in which the head bends ventrally toward the tail (Croll, 1975). Omega turns usually change the direction of locomotion to one directly opposite to the original trajectory (approximately 180°). Short reversals of one or two body bends lead to a relatively small (40° to 70°, respectively) change in direction of

locomotion (Gray et al., 2005; Zhao et al., 2003). Therefore, the suppression of head oscillations coupled to long reversals may allow the animal to engage in a more efficient escape response.

The *C. elegans* neural escape circuit is reminiscent of the neural escape circuit in flies. In the *Drosophila* escape response, the giant fiber (GF) neurons coordinate distinct motor programs: leg extension and wing depression, which are required for fast flight initiation (Hammond and O'Shea, 2007; Card and Dickinson, 2008). Fly GF interneurons make electrical synapses with the TTMn motor neurons, which control leg jump, and the PSI interneurons, which control wing depression (Tanouye and Wyman, 1980). Additional synaptic connectivity exists between PSI interneurons and the TTMn neurons that presumably contribute to a coordinated motor response (Phelan et al., 1996). Like the worm AVA neurons, the fly GF neurons control two distinct motor programs. Could tyramine play a role in the coordination of these motor programs in the fly escape response? Interestingly, tyramine appears to inhibit flight initiation (Brembs et al., 2007) and flies that have an excess of tyramine or lack the tyramine G protein-coupled receptor, TyR^{homo} do not jump as far as the wild-type in fly escape assays (Zumstein et al., 2004). These striking similarities between worms and flies suggest that tyramine may act as a conserved coordinator of motor programs in invertebrate escape responses.

EXPERIMENTAL PROCEDURES

Genetic Screen, Mapping, and Cloning of LGC-55

All strains were cultured at 22°C on NGM agar plates with the *E. coli* strain OP50 as a food source. The wild-type strain was Bristol N2. All strains were obtained from the *C. elegans* genetics center (CGC) unless otherwise noted. Wild-type animals were mutagenized with 50 mM EMS (Brenner, 1974). Young adult F2 progeny of approximately 14,000 mutagenized F1 animals were washed twice with water and transferred to 40 mM tyramine plates. After 10 to 20 min animals that displayed sustained head or body movements were picked to single plates. Primary isolates were retested on 30 mM tyramine. Twelve mutants were isolated, of which only *zf11* and *zf53* were sensitive to the inhibitory effects on body movements but resistant to the inhibitory effects on head movements.

We mapped *lgc-55(zf11)* to LG V using the SNP mapping procedure as previously described (Wicks et al., 2001; Davis et al., 2005). Further, three factor mapping placed *lgc-55(zf11)* to the left of *rol-9* close to *unc-51*. Full-length *lgc-55* cDNA sequence was obtained from the expressed sequence tag (EST) clone yk1072c.07. Standard techniques for molecular biology were used. ClustalW alignments were carried out using MacVector software (Accelrys). The *lgc-55* deletion allele was obtained from National Bioresource Project and outcrossed four times.

All transgenic strains were obtained by microinjection of plasmid DNA into the germline. At least three independent transgenic lines were obtained and data are from a single representative line. An *lgc-55* rescue construct was made by cloning a *lgc-55* genomic fragment corresponding to nucleotide (nt) −2663 to +3895 relative to the translation start site into the EcoRV site in yk1072c.07. For muscle specific rescue an Acc65I/XhoI fragment containing the full-length *lgc-55* cDNA was cloned into pPD95.86 behind the *myo-3* promoter. A 2751 bp genomic fragment upstream of the *sra-11* translation start site was fused to the full-length *lgc-55* cDNA for expression of LGC-55 in the AVB, AIY and AIA (weakly), as well as to GFP for expression analysis. A PstI/Acc65I fragment from the vector pV6 containing the *glr-1* promoter was fused to the full-length *lgc-55* cDNA for expression of LGC-55 in head neurons including RMD, SMDD, and SMDV. A 3545 bp genomic fragment upstream *lim-4* translation start site was fused to the full-length *lgc-55* cDNA for expression of LGC-55 in RMD and other head neurons. LGC-55::GFP translational fusion constructs were made by cloning GFP into an engineered AscI restriction in the genomic rescuing construct in the sequence encoding the intracellular loop between TM3 and TM4 (Figure 2C). Transgenic animals for cell specific rescue experiments were made by co-injecting genomic, LGC-55::GFP, *myo-3*::LGC-55, *sra-11*::LGC-55, *glr-1*::LGC-55 or *lim-4*::LGC-55 plasmids at 20 ng/μl along with the *lin-15* rescuing plasmid pL15EK at 80 ng/μl into *lgc-55(tm2913); lin15(n765ts)* animals. *lgc-55::gfp* and *lgc-55::mCherry* transcriptional fusion constructs were made by cloning a genomic fragment corresponding to nt −2663 to +3859 relative to the translational start site into the following vectors: pPD95.70 (GFP) and pPD95.70Cherry (mCherry). The membrane targeting signal sequence corresponding to nt +4 to +48 relative to the *lgc-55* translational start site was removed using site directed mutagenesis. GFP and mCherry constructs were microinjected along with the *lin-15* rescuing plasmid, pL15EK, at 80 ng/μl into *lin15(n765ts)* animals.

Cell Identification

Identifications of cells that expressed the *lgc-55::mCherry* reporter were based on cell body positions, axon morphologies, and coexpression with previously described cell specific GFP markers. Strains containing the following fusion genes were used to confirm cell identification: IL1: *sEx15005* (*y111b2a.8*::GFP), AVB: *otIs123* (*sra-11*::GFP), RMD, SMDD, SMDV: *kyIs29* (*glr-1*::GFP) and *nuIs25* (*glr-1*::GFP), and ALN, SDQ: *otIs107* (*ser-2*::GFP). All strains were examined for co-expression of GFP and mCherry by fluorescence microscopy.

Behavioral Assays

All behavioral analysis was performed with young adult animals (24 hr post-L4) at room temperature (22°C–24°C); different genotypes were scored in parallel, with the researcher blinded to the genotype. To quantify tyramine resistance, young adult animals were transferred to agar plates supplemented with 30 mM tyramine and the percentage of immobilized animals was scored every minute for a 20 min period. Body and head movements were scored separately. Body movement was defined as sustained locomotion for more than 5 s, and head movement was defined as sustained lateral swings of the head (anterior to the posterior pharyngeal bulb) only. Wild-type animals paralyzed on 30 mM tyramine within 3–5 min. Tyramine plates were prepared by autoclaving 1.7% agar in water, cooling to ~55°C and adding glacial acetic acid to a concentration of 2 mM and tyramine-HCl (Sigma) to a concentration of 30 mM.

To quantify the effect of tyramine on backward locomotion, animals were transferred in a small drop of water to agar plates with or without 30 mM tyramine (tyramine free plates were made as described above, without the addition of tyramine). The drop of liquid was quickly dried with a KimWipe, with care taken not to disturb the animal. Once the spot was dry, the animals were filmed using an Imaging Source DMK 21F04 firewire camera and Astro IIDC software, for 5 min or until the animal became paralyzed. The length of each reversal was quantified by counting the number of backward body bends. A backward body bend was defined as half of a sine wave and quantified by counting the number of bends made in the posterior body region during backward runs. The data represent the longest average reversal made within the time interval.

Spontaneous reversal frequency was scored on unseeded NGM agar. Animals were transferred from their culture plate to an unseeded plate and allowed to crawl away from any food that might have been transferred. The animals were then gently transferred without food to another unseeded plate and allowed to recover for 1 min. After the recovery period the animals were filmed for 3 min. The reversal frequency was determined as described in Tsalik et al. (2003), and reversal length was scored according to Gray et al. (2005). Animals that crawled to the edge of the plate during filming were discarded. To quantify backward locomotion in response to touch, animals were touched gently with an eyelash posterior to the pharynx and the number of backward body bends made in response to the touch was counted. The suppression of head oscillations was scored as described by Alkema et al. (2005).

Mosaic Analysis

Strains used for mosaic analysis (QW231 and QW232) were made by coinjecting *myo-3*::GFP (50 ng/μl), *lgc-55*::mCherry (30 ng/μl), the *lgc-55* rescuing construct (20ng/μl), and *lin-15* rescuing plasmid pL15EK (80 ng/μl) into *lgc-55(tm2913); lin15(n765ts)* animals. To facilitate the identification of animals that lost the

extrachromosomal array in the AB lineage, we selected multivulva (Muv) animals that expressed *myo-3*::GFP. Animals that lost the extragenic array the P1 lineage were selected by picking non-Muv animals that did not express *myo-3*::GFP. Animals that lost the rescuing array in either AB or P1 lineages and nonmosaic controls were tested for the suppression of head oscillations, head paralysis, and backward locomotion on exogenous tyramine as described above. Once behavioral assays were completed animals were mounted and examined for the presence of GFP and mCherry using fluorescence microscopy to confirm expression of the array in the appropriate cell type. Animals not expressing the array in all neck muscle or all head neurons were discarded.

Electrophysiology of LGC-55

An EagI/XhoI fragment containing the full length LGC-55 cDNA, including the 5′ and 3′ UTRs was cloned into the EagI/XhoI site of the vector pSGEM for oocyte expression. Capped RNA was prepared using T7 polymerase from Promega. Stage V and VI oocytes from *X. laevis* were injected with ~50 ng of cRNA. Two electrode voltage clamp experiments were preformed 2–3 days post injection at room temperature (22°C–24°C). The standard bath solution for dose response and control experiments was ND96: 96 mM NaCl, 2 mM KCl, 1.8 mM $CaCl_2$, 1 mM $MgCl_2$, 5 mM HEPES. For dose response experiments, oocytes were voltage clamped at −60 mV and were subjected to a 10 s application of neurotransmitter (1–1000 μM, in ND96) with 2–3 min washes between each application. All dose response data were normalized to the mean maximum current observed for tyramine. Data were gathered in 12 independent experiments for each neurotransmitter (totaling 31 eggs), using oocytes from different frogs. Data were consistent between the different batches of oocytes and represent the mean of at least four recordings for each dose of neurotransmitter.

The reversal potential of LGC-55 expressing oocytes was first determined in standard ND96 (as above). For the sodium permeability test, we substituted 96 mM NMDG for NaCl. The Cl^- permeability test was preformed in 10% NaCl (9.6 mM NaCl, 86.4 mM sodium gluconate, 2 mM KCl, 1.8 mM $CaCl_2$, 1 mM $MgCl_2$, 5mM HEPES). All points represent the response to an application of 10 μM TA for 10 s at the indicated holding potentials. Data were normalized to the tyramine current at −60 mV and averaged for 4–5 oocytes per data point. We used 3 M KCl filled electrodes with a resistance between 1 and 4 MΩ. We used agarose bridges to minimize liquid junction potentials and liquid junction potentials occurring at the tip of the recording electrodes were corrected prior to recording. Currents were recorded using Warner Instrument OC-725 two-electrode voltage clamp (TEVC) and data were acquired with Digidata 1322A using pClamp 9 (Axon Instruments). Normalized dose response data were fit to the Hill equation $\log(\theta/1\text{-}\theta) = n\log[L] - n\log K_A$. Reversal potential ($E_{rev}$) was calculated by determining the x intercept of the linear regression line of each I–V curve and averaged for 4–5 oocytes. Whole-cell voltage-clamp recordings of *C. elegans* muscle cells were performed as previously described in Francis and Maricq (2006). In short, recording pipettes were filled with an intracellular solution of 25 mM KCl and 115 mM K-gluconate. Muscle cells were voltage clamped at −60 mV and 200 μM tyramine was pressure applied for 250 ms. The reversal potential of LGC-55 in *C. elegans* body wall muscle was determined using voltage steps in 20 mV increments. Data were normalized to the I_{max} for each animal and averaged across 3 to 4 animals. Curve fitting and statistical analyses were performed with Prism version 5.0a for Mac OS X (GraphPad Software).

SUPPLEMENTAL DATA

The Supplemental Data include six figures and five movies and can be found with this article online at http://www.neuron.org/supplemental/S0896-6273(09)00294-3.

ACKNOWLEDGMENTS

We would like to thank Andrew Fire for GFP vectors, Yuji Kohara for cDNA clones, the *Caenorhabditis* Genetics Center (CGC) for worm strains, the National Bioresource Project for the *lgc-55* deletion mutant, Jennifer Ziegenfuss for help with the genetic screen, Bill Kobertz, Steven Gage, and Karen Mruk for help with the *Xenopus* oocyte experiments, David Hall and Zeynep Altun for help with cell identification, Villu Maricq for *glr-1* promoter constructs, Niels Ringstad, Namiko Abe, and Bob Horvitz for sharing unpublished results, Vivian Budnik and Scott Waddell for critically reading the manuscript. This research was supported by a grant from the Worcester Foundation (M.J.A.) and grant GM084491 from the National Institute of Health (M.J.A.).

Accepted: April 8, 2009
Published: May 27, 2009

REFERENCES

Alkema, M.J., Hunter-Ensor, M., Ringstad, N., and Horvitz, H.R. (2005). Tyramine functions independently of octopamine in the *Caenorhabditis elegans* nervous system. Neuron *46*, 247–260.

Allen, M.J., Godenschwege, T.A., Tanouye, M.A., and Phelan, P. (2006). Making an escape: development and function of the *Drosophila* giant fibre system. Semin. Cell Dev. Biol. *17*, 31–41.

Altun-Gultekin, Z., Andachi, Y., Tsalik, E.L., Pilgrim, D., Kohara, Y., and Hobert, O. (2001). A regulatory cascade of three homeobox genes, *ceh-10, ttx-3* and *ceh-23*, controls cell fate specification of a defined interneuron class in *C. elegans*. Development *128*, 1951–1969.

Bamber, B.A., Beg, A.A., Twyman, R.E., and Jorgensen, E.M. (1999). The *Caenorhabditis elegans unc-49* locus encodes multiple subunits of a heteromultimeric GABA receptor. J. Neurosci. *19*, 5348–5359.

Barron, G.L. (1977). The Nematode-Destroying Fungi. Topics in Mycobiology, No. 1 (Guelph, ON: Canadian Biological Publications).

Betz, H. (1990). Ligand-gated ion channels in the brain: the amino acid receptor superfamily. Neuron *5*, 383–392.

Blenau, W., Balfanz, S., and Baumann, A. (2000). Amtyr1: characterization of a gene from honeybee (*Apis mellifera*) brain encoding a functional tyramine receptor. J. Neurochem. *74*, 900–908.

Blumenthal, E.M. (2005). Modulation of tyramine signaling by osmolality in an insect secretory epithelium. Am. J. Physiol. Cell Physiol. *289*, C1261–C1267.

Borowsky, B., Adham, N., Jones, K.A., Raddatz, R., Artymyshyn, R., Ogozalek, K.L., Durkin, M.M., Lakhlani, P.P., Bonini, J.A., Pathirana, S., et al. (2001). Trace amines: identification of a family of mammalian G protein-coupled receptors. Proc. Natl. Acad. Sci. USA *98*, 8966–8971.

Brembs, B., Christiansen, F., Pfluger, H.J., and Duch, C. (2007). Flight initiation and maintenance deficits in flies with genetically altered biogenic amine levels. J. Neurosci. *27*, 11122–11131.

Brenner, S. (1974). The genetics of *Caenorhabditis elegans*. Genetics *77*, 71–94.

Card, G., and Dickinson, M. (2008). Performance trade-offs in the flight initiation of *Drosophila*. J. Exp. Biol. *211*, 341–353.

Chalfie, M., and Sulston, J. (1981). Developmental genetics of the mechanosensory neurons of *Caenorhabditis elegans*. Dev. Biol. *82*, 358–370.

Chalfie, M., Sulston, J.E., White, J.G., Southgate, E., Thomson, J.N., and Brenner, S. (1985). The neural circuit for touch sensitivity in *Caenorhabditis elegans*. J. Neurosci. *5*, 956–964.

Chalfie, M., Tu, Y., Euskirchen, G., Ward, W.W., and Prasher, D.C. (1994). Green fluorescent protein as a marker for gene expression. Science *263*, 802–805.

Chronis, N., Zimmer, M., and Bargmann, C.I. (2007). Microfluidics for in vivo imaging of neuronal and behavioral activity in *Caenorhabditis elegans*. Nat. Methods *4*, 727–731.

Cole, S.H., Carney, G.E., McClung, C.A., Willard, S.S., Taylor, B.J., and Hirsh, J. (2005). Two functional but noncomplementing *Drosophila* tyrosine decarboxylase genes: distinct roles for neural tyramine and octopamine in female fertility. J. Biol. Chem. *280*, 14948–14955.

Cowan, W.M., Südhof, T.C., and Stevens, C.F. (2001). Synapses (Baltimore, MD: Johns Hopkins University Press).

Croll, N.A. (1975). Integrated behavior in the feeding phase of Ceanorhabditis *elegans* (Nematoda). J. Zool. *176*, 159–176.

Davis, M.W., Hammarlund, M., Harrach, T., Hullett, P., Olsen, S., and Jorgensen, E.M. (2005). Rapid single nucleotide polymorphism mapping in *C. elegans*. BMC Genomics *6*, 118.

Edwards, D.H., Yeh, S.R., Musolf, B.E., Antonsen, B.L., and Krasne, F.B. (2002). Metamodulation of the crayfish escape circuit. Brain Behav. Evol. *60*, 360–369.

Francis, M.M., and Maricq, A.V. (2006). Electrophysiological analysis of neuronal and muscle function in *C. elegans*. Methods Mol. Biol. *351*, 175–192.

Gray, J.M., Hill, J.J., and Bargmann, C.I. (2005). A circuit for navigation in *Caenorhabditis elegans*. Proc. Natl. Acad. Sci. USA *102*, 3184–3191.

Green, W.N., and Wanamaker, C.P. (1997). The role of the cystine loop in acetylcholine receptor assembly. J. Biol. Chem. *272*, 20945–20953.

Grutter, T., de Carvalho, L.P., Dufresne, V., Taly, A., Edelstein, S.J., and Changeux, J.P. (2005). Molecular tuning of fast gating in pentameric ligand-gated ion channels. Proc. Natl. Acad. Sci. USA *102*, 18207–18212.

Hall, D., and Altun, Z.F. (2007). *C. elegans* Atlas (Cold Spring Harbor, NY: Cold Spring Harbor Laboratory Press).

Hammond, S., and O'Shea, M. (2007). Escape flight initiation in the fly. J. Comp. Physiol. A Neuroethol. Sens. Neural Behav. Physiol. *193*, 471–476.

Hart, A.C., Sims, S., and Kaplan, J.M. (1995). Synaptic code for sensory modalities revealed by *C. elegans* GLR-1 glutamate receptor. Nature *378*, 82–85.

Henwood, R.W., Boulton, A.A., and Phillis, J.W. (1979). Iontophoretic studies of some trace amines in the mammalian CNS. Brain Res. *164*, 347–351.

Isaac, R.E., MacGregor, D., and Coates, D. (1996). Metabolism and inactivation of neurotransmitters in nematodes. Parasitology *113* (*Suppl*), S157–S173.

Jones, A.K., and Sattelle, D.B. (2008). The cys-loop ligand-gated ion channel gene superfamily of the nematode, *Caenorhabditis elegans*. Invert. Neurosci. *8*, 41–47.

Karlin, A., and Akabas, M.H. (1995). Toward a structural basis for the function of nicotinic acetylcholine receptors and their cousins. Neuron *15*, 1231–1244.

Katz, P.S., Getting, P.A., and Frost, W.N. (1994). Dynamic neuromodulation of synaptic strength intrinsic to a central pattern generator circuit. Nature *367*, 729–731.

Korn, H., and Faber, D.S. (2005). The Mauthner cell half a century later: a neurobiological model for decision-making? Neuron *47*, 13–28.

Marder, E., and Bucher, D. (2001). Central pattern generators and the control of rhythmic movements. Curr. Biol. *11*, R986–R996.

Maricq, A.V., Peckol, E., Driscoll, M., and Bargmann, C.I. (1995). Mechanosensory signalling in *C. elegans* mediated by the GLR-1 glutamate receptor. Nature *378*, 78–81.

McIntire, S.L., Jorgensen, E., Kaplan, J., and Horvitz, H.R. (1993). The GABAergic nervous system of *Caenorhabditis elegans*. Nature *364*, 337–341.

Mellem, J.E., Brockie, P.J., Madsen, D.M., and Maricq, A.V. (2008). Action potentials contribute to neuronal signaling in *C. elegans*. Nat. Neurosci. *11*, 865–867.

Miller, G.M., Verrico, C.D., Jassen, A., Konar, M., Yang, H., Panas, H., Bahn, M., Johnson, R., and Madras, B.K. (2005). Primate trace amine receptor 1 modulation by the dopamine transporter. J. Pharmacol. Exp. Ther. *313*, 983–994.

Monastirioti, M., Linn, C.E., Jr., and White, K. (1996). Characterization of *Drosophila* tyramine beta-hydroxylase gene and isolation of mutant flies lacking octopamine. J. Neurosci. *16*, 3900–3911.

Mullen, G.P., Mathews, E.A., Saxena, P., Fields, S.D., McManus, J.R., Moulder, G., Barstead, R.J., Quick, M.W., and Rand, J.B. (2006). The *Caenorhabditis elegans* snf-11 gene encodes a sodium-dependent GABA transporter required for clearance of synaptic GABA. Mol. Biol. Cell *17*, 3021–3030.

Nusbaum, M.P., and Beenhakker, M.P. (2002). A small-systems approach to motor pattern generation. Nature *417*, 343–350.

Ohta, H., Utsumi, T., and Ozoe, Y. (2003). B96Bom encodes a *Bombyx mori* tyramine receptor negatively coupled to adenylate cyclase. Insect Mol. Biol. *12*, 217–223.

Okkema, P.G., Harrison, S.W., Plunger, V., Aryana, A., and Fire, A. (1993). Sequence requirements for myosin gene expression and regulation in *Caenorhabditis elegans*. Genetics *135*, 385–404.

Ortells, M.O., and Lunt, G.G. (1995). Evolutionary history of the ligand-gated ion-channel superfamily of receptors. Trends Neurosci. *18*, 121–127.

Paton, W.D. (1958). Central and synaptic transmission in the nervous system; pharmacological aspects. Annu. Rev. Physiol. *20*, 431–470.

Phelan, P., Nakagawa, M., Wilkin, M.B., Moffat, K.G., O'Kane, C.J., Davies, J.A., and Bacon, J.P. (1996). Mutations in shaking-B prevent electrical synapse formation in the *Drosophila* giant fiber system. J. Neurosci. *16*, 1101–1113.

Ranganathan, R., Cannon, S.C., and Horvitz, H.R. (2000). MOD-1 is a serotonin-gated chloride channel that modulates locomotory behaviour in *C. elegans*. Nature *408*, 470–475.

Rex, E., and Komuniecki, R.W. (2002). Characterization of a tyramine receptor from *Caenorhabditis elegans*. J. Neurochem. *82*, 1352–1359.

Rex, E., Hapiak, V., Hobson, R., Smith, K., Xiao, H., and Komuniecki, R. (2005). TYRA-2 (F01E11.5): a *Caenorhabditis elegans* tyramine receptor expressed in the MC and NSM pharyngeal neurons. J. Neurochem. *94*, 181–191.

Roeder, T., Seifert, M., Kahler, C., and Gewecke, M. (2003). Tyramine and octopamine: antagonistic modulators of behavior and metabolism. Arch. Insect Biochem. Physiol. *54*, 1–13.

Sagasti, A., Hobert, O., Troemel, E.R., Ruvkun, G., and Bargmann, C.I. (1999). Alternative olfactory neuron fates are specified by the LIM homeobox gene *lim-4*. Genes Dev. *13*, 1794–1806.

Saudou, F., Amlaiky, N., Plassat, J.L., Borrelli, E., and Hen, R. (1990). Cloning and characterization of a *Drosophila* tyramine receptor. EMBO J. *9*, 3611–3617.

Shaner, N.C., Campbell, R.E., Steinbach, P.A., Giepmans, B.N., Palmer, A.E., and Tsien, R.Y. (2004). Improved monomeric red, orange and yellow fluorescent proteins derived from Discosoma sp. red fluorescent protein. Nat. Biotechnol. *22*, 1567–1572.

Tanouye, M.A., and Wyman, R.J. (1980). Motor outputs of giant nerve fiber in *Drosophila*. J. Neurophysiol. *44*, 405–421.

Thorn, R.G., and Barron, G.L. (1984). Carnivorous mushrooms. Science *224*, 76–78.

Tsalik, E.L., Niacaris, T., Wenick, A.S., Pau, K., Avery, L., and Hobert, O. (2003). LIM homeobox gene-dependent expression of biogenic amine receptors in restricted regions of the *C. elegans* nervous system. Dev. Biol. *263*, 81–102.

Weber, W. (1999). Ion currents of *Xenopus laevis* oocytes: state of the art. Biochim. Biophys. Acta *1421*, 213–233.

White, J.G., Southgate, E., Thomson, J.N., and Brenner, S. (1986). The structure of the of the nervous system of the nematode *Caenorhabditis elegans*. Philos. Trans. R. Soc. Lond. B Biol. Sci. *314*, 1–340.

Wicks, S.R., Yeh, R.T., Gish, W.R., Waterston, R.H., and Plasterk, R.H. (2001). Rapid gene mapping in *Caenorhabditis elegans* using a high density polymorphism map. Nat. Genet. *28*, 160–164.

Wragg, R.T., Hapiak, V., Miller, S.B., Harris, G.P., Gray, J., Komuniecki, P.R., and Komuniecki, R.W. (2007). Tyramine and octopamine independently inhibit serotonin-stimulated aversive behaviors in *Caenorhabditis elegans* through two novel amine receptors. J. Neurosci. *27*, 13402–13412.

Zhao, B., Khare, P., Feldman, L., and Dent, J.A. (2003). Reversal frequency in *Caenorhabditis elegans* represents an integrated response to the state of the animal and its environment. J. Neurosci. *23*, 5319–5328.

Zheng, Y., Brockie, P.J., Mellem, J.E., Madsen, D.M., and Maricq, A.V. (1999). Neuronal control of locomotion in *C. elegans* is modified by a dominant mutation in the GLR-1 ionotropic glutamate receptor. Neuron *24*, 347–361.

Zhu, Z.T., Munhall, A.C., and Johnson, S.W. (2007). Tyramine excites rat subthalamic neurons in vitro by a dopamine-dependent mechanism. Neuropharmacology *52*, 1169–1178.

Zumstein, N., Forman, O., Nongthomba, U., Sparrow, J.C., and Elliott, C.J. (2004). Distance and force production during jumping in wild-type and mutant *Drosophila melanogaster*. J. Exp. Biol. *207*, 3515–3522.